Available online at www.sciencedirect.com
ScienceDirect
Earth and Planetary Science Letters 258 (2007) 207–218
EPSL
www.elsevier.com/locate/epsl

Small pressure drop triggered near a fault by small teleseismic waves

M.L. Doan [a,*], F.H. Cornet [b,1]

[a] Earth & Planetary Science Department, Earth & Marine Sciences Building, University of Santa Cruz, 1156, High Street, CA 95064, Santa Cruz, United States
[b] Department of Seismology, Institut de Physique du Globe de Paris, Casier 89, 4, place Jussieu, 75005, Paris, France

Received 27 October 2006; received in revised form 22 January 2007; accepted 16 March 2007
Available online 28 March 2007
Editor: C.P. Jaupart

Abstract

We describe a pressure transient triggered near an active fault by seismic waves generated more than 10 000 km away during the 2003 $M_w = 7.8$ Rat Island earthquake. In contrast with previous similar observations, the pressure drop occurs simultaneously with the arrival of S waves, and not during the passage of the Rayleigh waves that have larger amplitudes and smaller frequencies. This small 60 Pa drop is compatible with a small slip on the fault, which induced either dilatant damage or a transient disruption in the impermeable barrier the fault constitutes.

Keywords: dynamic triggering; pore pressure monitoring; active fault long-term monitoring; borehole instrumentation

Water-level changes induced by remote earthquakes have been documented since the Alaskan Earthquake of 1964 [1]. Montgomery and Manga [2] review dozens of such events and compare their distance to the epicenter to the magnitude of the corresponding earthquake. All their data lie above a line that corresponds to a volumetric strain equal to 10^{-8}, and they attribute this limit to instrumentation resolution. Such small a threshold suggests that some of these disturbances are dynamically triggered.

High frequency data shows that these disturbances can be concurrent with the passage of the Rayleigh waves [3]. These pressure changes are often interpreted as changes in permeability, which has also been shown to be altered by seismic waves [4]. Interestingly, triggered seismicity can also start from Rayleigh waves arrival [5]. The relationship between the two triggering phenomena is still not clear.

The Corinth Rift Laboratory is devoted to the joint observation of deformation and fluid pressure in a seismically active area. In addition to pressure data, seismometers and strainmeters monitor the Rift deformation. After a presentation of the borehole intersecting the Aigio fault, we describe the pressure drop induced by the 2003 Rat Island earthquake together with data from a seismometer and a dilatometer located 10 km away from the well. We check the absence of artifact due to the instrumentation or to a change in oceanic loading.

* Corresponding author. Tel.: +1 831 459 1311; fax: +1 831 459 3074.
E-mail addresses: mdoan@pmc.ucsc.edu (M.L. Doan), cornet@ipgp.jussieu.fr (F.H. Cornet).
[1] Tel.: +33 1 44 27 38 97; fax: +33 1 44 27 38 94.

0012-821X/$ - see front matter © 2007 Elsevier B.V. All rights reserved.
doi:10.1016/j.epsl.2007.03.036

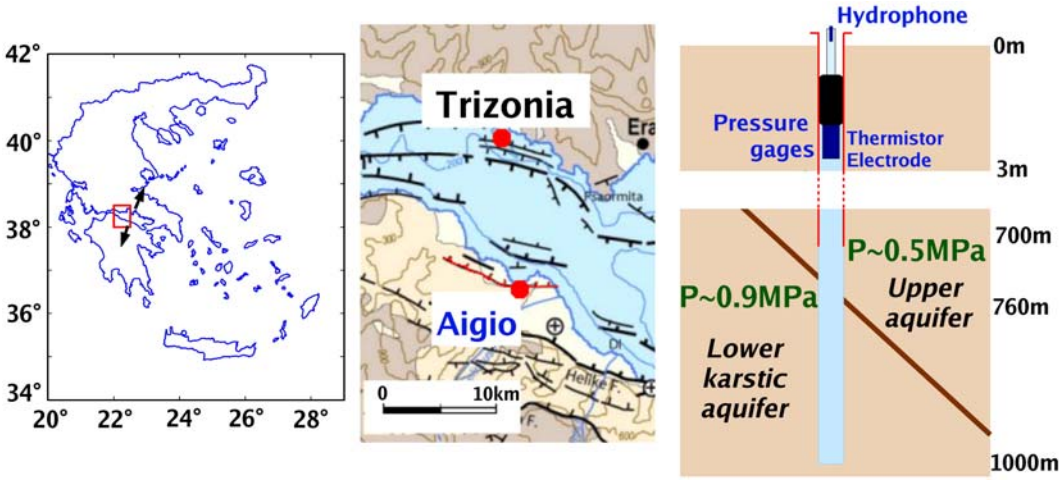

Fig. 1. (Left) The Corinth Rift, Greece, opens at a rate of 1.5 cm/yr. (Middle) In its western part, this activity is accompanied by intense faulting on its southern shore. We will focus on the Aigio fault, in the city of Aigio. (Right) The Aigio fault is intersected at 760 m by the deep Aigio borehole. The fault is surrounded by two aquifers decoupled from the surface by more than 300 m of clay and radiolarite: the upper fractured limestone aquifer with an overpressure of 0.5 MPa and the karstic lower aquifer, with an overpressure of 0.9 MPa. The difference in pressure implies that the fault is a hydraulic barrier. A pressure transducer has been installed at his wellhead. In addition to the pressure records, we consider the data from a hydrophone set up within the wellhead and from a set of seismometer and dilatometer located on Trizonia Island, some 10 km north to the borehole.

Finally, we propose several interpretations for the pressure drop.

1. The Corinth Rift and the Deep Geophysical LABoratory

The Corinth Rift is one of the most active extensional regions in Europe. This 130 km long, 20 km wide gulf separates continental Greece from Peloponnesus (Fig. 1). Its extension rate reaches locally 1.5 cm/yr, accompanied by large earthquakes like the M_s=6.2, June 15th, 1995 Aigio earthquake [6]. This earthquake caused up to 3 cm of surface displacement along the Aigio fault on the south-western shore of the Gulf [7], although the main rupture zone was slightly north to the Gulf, on a shallowly dipping fault.

This suggests that the fault may be creeping. GPS data over 11 years ([8], Fig. 4) show that a horizontal movement of 4 mm/yr has been monitored across the Aigio fault. This is similar to the slip rate along the fault obtained by paleoseimologic studies [9]. This motivated the choice of the Aigio fault as the site of the Deep Geophysical LABoratory project (DGLab).

The 1000 m deep AIG10 borehole intersects the active Aigio fault at 760 m (Fig. 1). The well is cased down to 700 m. Cores and logging images provide a precise description of the formations below the casing. The Aigio fault is smeared by a 1 m thick layer of clayish material that acts as a hydraulic barrier separating two different limestone aquifers [10]. The upper one has an overpressure equal to 0.5 MPa. Its hydraulic conductivity has been estimated to be 8×10^{-8} m/s through production test [11]. The lower aquifer is an artesian karst, with an overpressure of 0.87 MPa. Its high hydraulic conductivity ($1.3\pm0.2\times10^{-5}$ m/s) is caused by the cavities of metric size intersected by the borehole.

Its instrumentation was installed in September 2003 (Fig. 1). This includes a high-precision absolute pressure transducer, which operates at a sampling rate of 1/8 Hz with a resolution of 10 Pa. Another major sensor is a hydrophone, sampled at 2.5 kHz, that monitors the local high frequency microseismic activity. The installation was operating from fall 2003 to the end of 2004.

Three months after the installation, the wellhead pressure stabilized to about 0.85 MPa, a value very close to the original lower karstic aquifer overpressure (Fig. S2). As expected from the high permeability and storativity of the karst, the recorded pressure variations reflect the changes in the karstic aquifer.

2. Hydraulic transients triggered by teleseisms

2.1. Recordings of the 2003 Rat Island earthquake

On November 17, 2003, a M_w=7.8 earthquake occurred below Rat Island in the Aleutian archipelago, some 10 000 km away from the AIG10 borehole. The piezometer gave excellent recordings of the seismic waves (Figs. 2 and 4), superimposed with a 60 Pa drop.

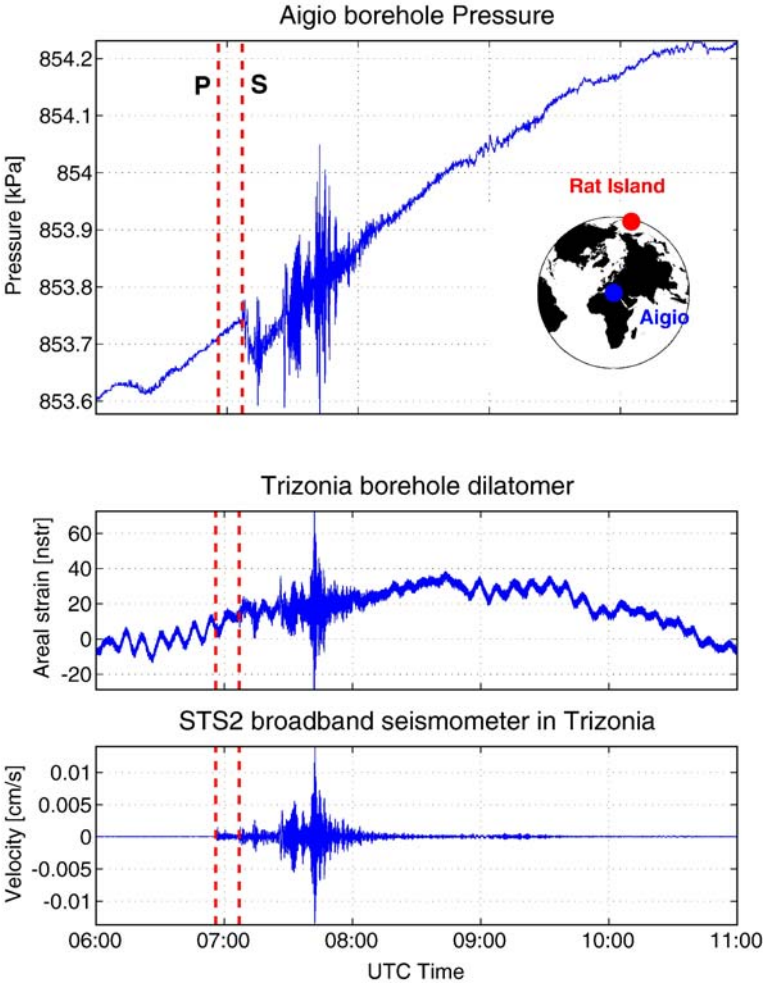

Fig. 2. (Top) The seismic waves generated by the M_w 7.8, November 17th, 2003 Rat Island earthquake are recorded by the pressure transducer of the AIG10 borehole. In addition to the seismic oscillations, a transient pressure drop is visible. The long-term trend is due to tidal variations. Red dashed lines show the arrival time of P and S waves predicted by the program ak135ttimes. (Middle) Recording of the same seismic waves by the borehole dilatometer on Trizonia Island (Fig. 1). Short-term fluctuations induced by the seiches within the Gulf of Corinth are visible. No clear anomaly occurs during the passing of the waves. (Bottom) Recording of the same seismic waves by the broadband seismometer installed on Trizonia Island. (For interpretation of the references to colour in this figure legend, the reader is referred to the web version of this article.)

The drop lasts about 5 min and is followed by a recovery phase about 30 min long. This pressure drop corresponds to a volumetric dilation of 3.5×10^{-9} only.

Complementary information was provided by a STS-2 broadband seismometer and a Sacks–Evertson dilatometer (10^{-10} resolution) located on Trizonia Island, some 10 km to the north of AIG10 borehole (Fig. 1). All sensors record the teleseismic waves but only the AIG10 pressure gauge exhibits a transient.

Fig. 2 shows that the onset of the drop coincides with the arrival of S waves, and not with the passage of the Rayleigh waves as it is usually observed (for instance, all published triggering induced by the Sumatra earthquake occurred with the passing of the Rayleigh waves [12–14]). This suggests that the environment around the borehole was on the very verge of instability since the small S waves amplitude were able to trigger the hydraulic transient. The amplitude of the areal deformation of the S waves (periods of the order of 30 s) as recorded on the dilatometer is 5×10^{-9}, while the fluid pressure oscillations reach 50 Pa. The particle velocity amplitude is only 0.001 cm/s. The triggered anomaly of Fig. 2 is original by the smallness of its triggering waves, much smaller than the surface waves that usually trigger the seismicity and the hydraulic anomalies so far reported [2].

This pressure transient is coincidental with a sharp signal recorded on the hydrophone located just above

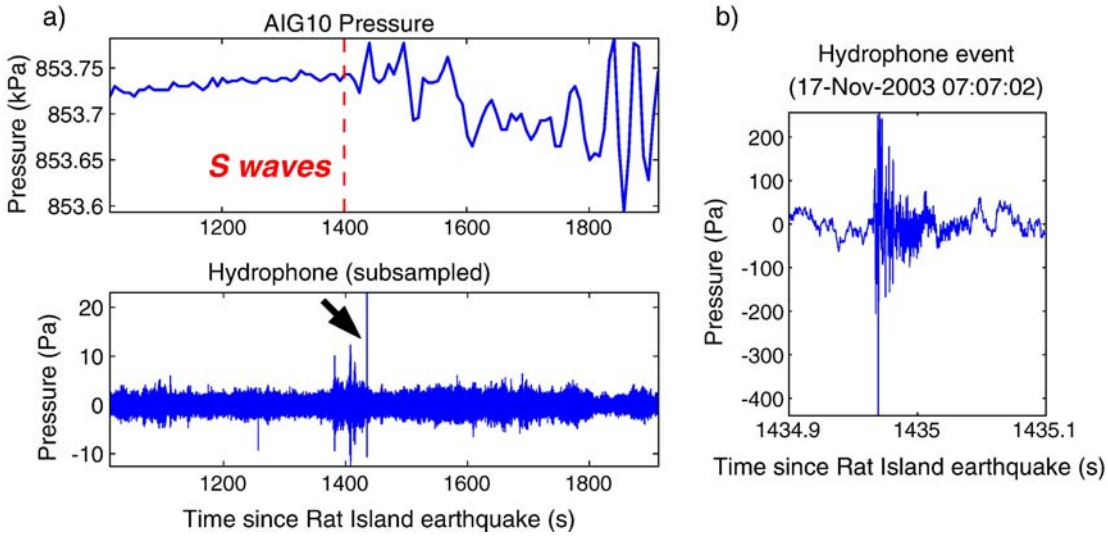

Fig. 3. High frequency event recorded on the hydrophone located at the wellhead of the AIG10 borehole (Fig. 1). The event occurs a few seconds after the first arrival of the S waves and coincides with the onset of the pressure drop. The event duration is only 100 ms long and there are resonant oscillations at 850 Hz.

the well. A zoom of this signal is presented in Fig. 3. It occurs at the beginning of the pressure drop. The signal is quasi-monochromatic with a peak frequency at 850 Hz that possibly corresponds to a resonance of the metallic structure installed at the wellhead. However, similar events have been recorded during the year of operation, most of them being not correlated with a pressure transient. They might be related to the expected creep on the Aigio fault. However, the relationship of the single hydrophone signal with the downhole evolution cannot be assessed. This is regrettable since it is the only complementary anomalous signal observed at that time on the sensors surrounding the piezometer.

2.2. Assessment of signal reliability

We will compare the high frequency pressure oscillations to the dilatometer data to check the good behavior of the sensor. We will also correct the dependence of the hydraulic pressure on external loadings (Earth tides and oceanic load) and check that the drop is not due to a change in these loads.

2.2.1. Recording of seismic oscillations

Seismic waves are obtained by high-pass filtering the data of the pressure gauge p and of the dilatometer data ε_h (Fig. 4). Both data sets are in excellent agreement, as the relationship $p=(-10\ \mathrm{GPa})\times\varepsilon_h$ holds as long as the Nyquist frequency criterion is satisfied. That means that we consider only periods greater than $2\times 8\ \mathrm{s}=16\ \mathrm{s}$. With seismic velocities of at least 3 km/s, the wavelength of the seismic waves is of at least 48 km. As Trizonia and Aigio are separated by only 10 km, the two sensors record similar seismic waves.

Fig. 4 shows two surprising trends: first, there is a negative sign between the pressure signal and the dilatometer (with a contraction denoted as positive); second, the pressure sensor is also sensitive to shear waves.

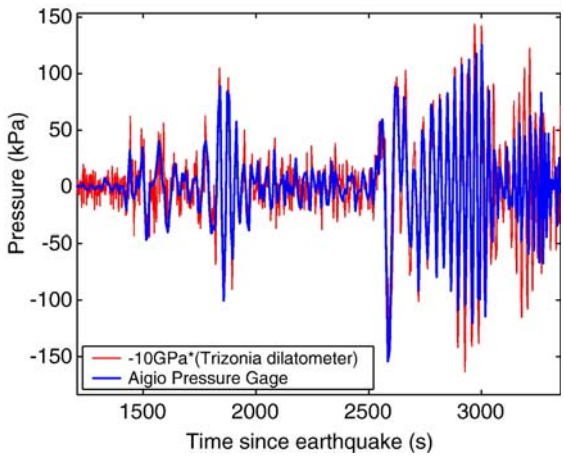

Fig. 4. Comparison of the data from pressure gauge in Aigio and the Sacks–Evertson dilatometer of Trizonia. The dilatometer data has been multiplied by a factor equal to −10 before displaying. Both are high-pass filtered to highlight the seismic waves the sensor felt. The time span shown is when the frequency of the seismic oscillation is below the Nyquist frequency of the pressure transducer, 1/16 Hz.

The opposite sign between the pressure signal at Aigio and the dilatometer in Trizonia is due to the fact that teleseismic waves have a vertical incidence. P waves are compression waves, with compression longitudinal to their propagation direction. Hence the volumetric strain, to which the pressure is sensitive, is dominated by vertical deformation, whereas the borehole dilatometer is only sensitive to the horizontal deformation. The relationship between the two data is:

$$K = \frac{\partial p}{\partial \varepsilon_h} = -3(BK_u)_a \frac{(1-2\nu_{ua})^2}{2\nu_{ut}} \quad (1)$$

where ν_{ut} is the undrained Poisson ratio for Trizonia soil and B, K_{ua} and ν_{ua} are respectively the Skempton coefficient, the undrained bulk modulus and the undrained Poisson ratio of the rock in Aigio. By taking the parameters obtained from the joint analysis of the Earth tides and the oceanic load ($(BK_u)_a$=17 GPa, ν_{ua}=0.2) and assuming ν_{ut}=0.25, we get a factor K=−26 GPa, of the same order of magnitude as the experimental value of −10 GPa. Notice that we did not have to resort to specific ground conditions, as horizontal fractures in [15].

In a pure poroelastic medium, the pressure is sensitive to volumetric strain only and not to shear strain. Is the fact that the pressure sensor records shear waves like S waves due to the presence of fractures that open when they are sheared? Fig. 2 shows that the dilatometer of Trizonia is also sensitive to shear waves. Fig. 4 shows that the Trizonia dilatometer records the same oscillations as the Aigio pressure sensor. Their sensitivity to the shear waves can therefore be attributed to the P–S conversion at the Earth surface rather than to local effects like fracture compliance to shear stress.

We have checked that the instrument ran correctly during the recording of the pressure drop.

2.2.2. Removal of the external loads

As seen from the tidal analysis, the pressure signal reflects both the ground deformation and the oceanic load. Because of the proximity of the borehole to the seashore (500 m), the last effect accounts for as much as 50% of the tidal oscillations [16].

The sea level of the Gulf of Corinth is affected by stationary waves (seiches) within the Gulf. The Gulf resonates at two major periods: 40 min in the E–W direction and 5 min in the N–S direction. The resonances were excited by wind that day, as the dilatometer data of Fig. 2 shows. Is the observed drop simply a large 5-minute seiche?

We corrected this seiches effect with tide gauge data. First, the tidal variations are removed. The remaining oscillations of the pressure data are supposed to be induced by ocean load. They are then removed by subtracting tide gauge data with a proportionality factor determined by least-square inversion on a test period prior to the Aleutian event (Fig. 5). The seiches are corrected as the amplitude of the 40-minute oscillations is reduced but the observed 5-minute pressure drop remains.

Hence the pressure variation is neither an instrumental artifact, nor an indirect effect of the oceanic loading.

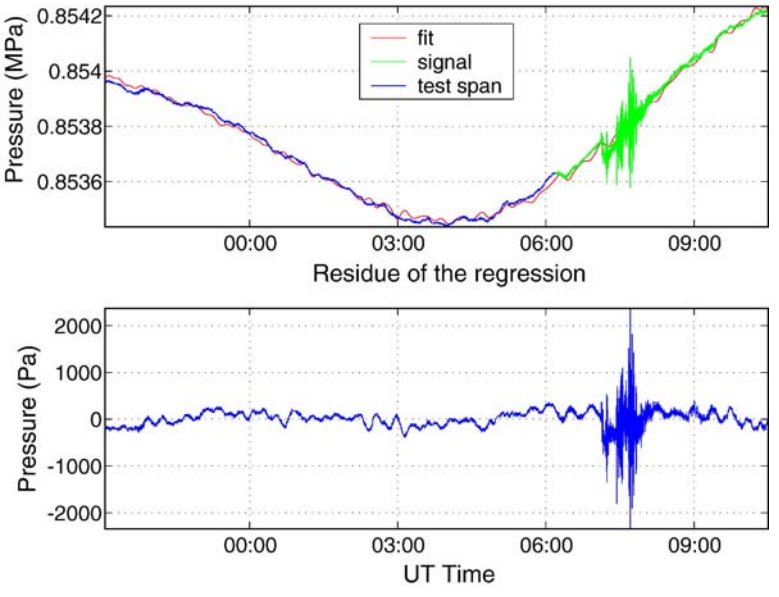

Fig. 5. Removing the effect of earth tides and oceanic loading flattens the long-term signal, and partially reduces the seiches. The anomaly is still clearly visible.

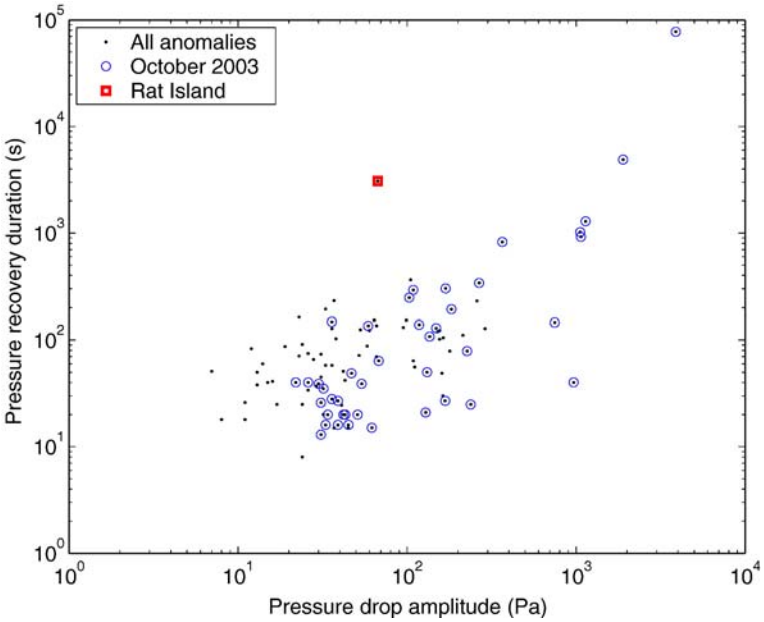

Fig. 6. Comparison of the amplitude of the drop and duration of recovery for hydraulic anomalies recorded in the AIG10 borehole during the year of operation of the instrumentation. The Rat Island drop has much larger duration if one discards the large anomalies that occurred during October 2003.

Something happened near the Aigio borehole. But is it induced by the seismic waves?

2.3. Comparison with other events

Numerous other hydraulic transients have been recorded on site. Is the pressure drop simultaneous with the arrival of the seismic waves by mere chance? To assess this possibility, we compare this transient with the other pressure transients recorded and describe what happened for other teleseismic events.

2.3.1. Other pressure transients

More than 100 short-term hydraulic changes have been recorded during the one year of operation of the pressure sensor. Most of them happened during the first month of recording, with a paroxysmal activity in the beginning of October 2003 (see Fig. S1). If we discard the events recorded at that time, each of the remaining pressure transients recorded has a short duration, with a decay and a recovery of the same duration of 2 min maximum (Fig. 6). By contrast, Fig. 2 shows a decay lasting 5 min and a recovery exceeding 30 min.

Several short pressure transients were recorded in the AIG10 borehole but none like the one of Fig. 2. The pressure drop we recorded is thus not an event which could have occurred at any time, including during the passing of the seismic waves.

2.3.2. Other triggered events

To identify pressure transients induced by seismic waves, we need to be able to separate low frequency pressure transients from high frequency seismic waves. Unfortunately, the sampling frequency is only 8 s, and only large and remote events have seismic waves with frequency low enough for the passing waves not being subsampled.

Among the teleseismic events listed in Table 1, only three events induced seismic waves with amplitude larger

Table 1
List of teleseisms felt by the pressure sensor and the peak-to-peak amplitude of the seismic waves, as recorded by the pressure sensor (only the order of magnitude is given since in most cases, the seismic oscillations are subsampled at the time of the maximum amplitude)

Earthquake	Maximum peak-to-peak amplitude	Triggering?
2003-09-25 Hokkaido $M=8.3$	500 Pa	No hydraulic anomaly
2003-11-17 Rat Island $M=7.8$	500 Pa	Hydraulic anomaly
2003-12-26 Bam $M=6.6$	50 Pa (data missing)	No hydraulic anomaly
2004-05-28 Iran $M=6.3$	150 Pa	No hydraulic anomaly
2004-09-05 Honshu $M=7.2$	200 Pa	No hydraulic anomaly
2004-12-26 Sumatra $M\geq 9$	2000 Pa (data missing)	Hydraulic anomaly

Only two of these events induced a hydraulic anomaly.

than 500 Pa as recorded in the pressure sensor in Aigio. In addition of the Rat Island earthquake, two additional large teleseismic events have been recorded by the permanent borehole instrumentation: the Hokkaido September 25th, 2003 earthquake that did not induce any pressure change, and the December 26th, 2004 Sumatra earthquake that did. Let us observe that the Hokkaido earthquake occurs only 24 h after the installation of the sensor. During the installation, the fault could not be sealed and the karstic aquifer emptied in the upper aquifer. The pressure took three months to stabilize. Only 24 h after the installation, the fluid pressure of each aquifer was still close to its initial values.

Fig. 7 shows the raw pressure record corresponding to the seismic waves of the Sumatra earthquake. The data is spoiled by recording difficulties resulting in an irregular sampling rate and the loss of about half the data. However, a 2-minute data sample around 01:47 UT exhibits oscillations well below the Nyquist frequency. Its mean value is about 50 Pa lower than the mean pressure value observed before the event. This indicates that a pressure drop occurred during the Rayleigh waves. But the precise complete time description of the pressure drop and the recovery period cannot be retrieved. Also, no hydrophone signal was available for this event. We cannot compare further the two triggered events.

That other teleseismic waves are coincidental with a pressure drop supports the hypothesis that the pressure drop is triggered by the seismic waves generated by the Rat Island earthquake.

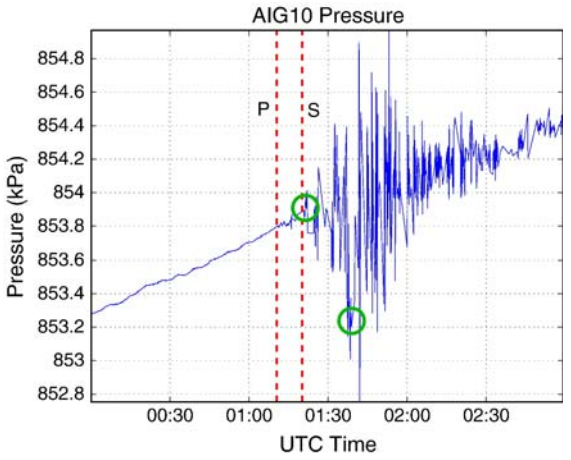

Fig. 7. Record of the pressure response to the seismic waves generated by the December 26th, 2004 Sumatra earthquake. The theoretical P and S waves arrival are denoted by dashed lines. Some samples miss because of acquisition problems but two points seem reliable. They correspond to two 2-minute continuous spans during which the correctly sampled variations are oscillating around a mean value whose coordinates are highlighted by circles. This event thus induced a hydraulic anomaly.

3. Possible mechanisms for the pressure drop

The absence of transients on the Trizonia sensors and the presence of the hydrophone signal hint that the cause of the pressure transient is local to the borehole. Two hypotheses can be formulated: the seismic waves disturbed a possible plug which could have formed inside the borehole during the crisis of October 2003 or the seismic waves disturbed the Aigio fault intersected by the AIG10 borehole.

3.1. A borehole related effect?

In October 2003, the recorded pressure exhibited large drops accompanied by an intense activity on the hydrophone installed at the wellhead (Fig. S1). Did the borehole collapse at that time, and is the transient related to a plug at the fault zone depth where the borehole is the weakest?

Several arguments let us think that the possible plug is not hydraulically significant. If it could clog the well, Fig. 1 shows that a plug at the fault zone would disconnect the surface pressure sensor from the bottom karst (about 0.9 MPa), and the sensor would record the pressure of the upper fractured aquifer (about 0.5 MPa). If the October 2003 crisis had installed an impermeable plug separating the two aquifers, the aquifer tapped by the pressure sensor would be different. But the tidal response of the well is the same before and after the October crisis (Fig. S1). Also after a 3 kPa decrease during the crisis, the pressure became similar to the 0.86 MPa recorded prior to the crisis. This suggests that even if the borehole partly collapsed on October 2003, it is not enough to disturb the hydraulic properties of the well.

Even if we suppose that an impermeable plug exists in the borehole and that we suppose that the seismic waves have disturbed the plug rather than the aquifers or the fault around the borehole, the data do not fit the expected behavior. We would expect the pressure to increase, varying from the low pressure of the fractured aquifer to the higher pressure in the karst. Yet the observed pressure evolution is a drop. We would expect a disturbance of the borehole to be instantaneously felt as the borehole is hydraulically very conducive, whereas the drop lasts 5 min. The slow recovery also suggests that the source is far from the borehole, not right in the borehole.

3.2. A fault related effect?

The Aigio fault is suspected to be creeping and easy to move. Can the pressure transient be due to a slip on

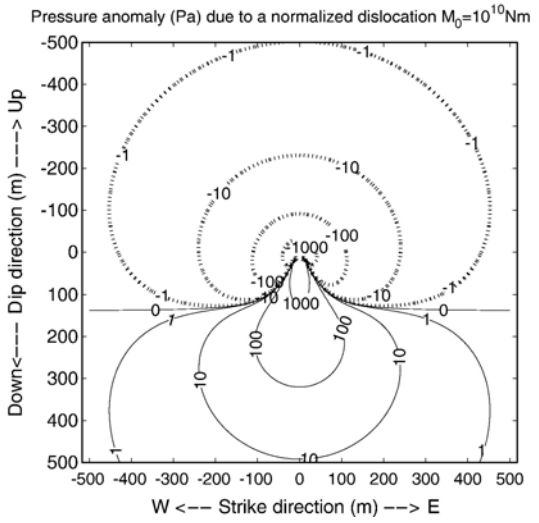

Fig. 8. Pressure induced at the borehole as a function of the slip location on the fault. We used a normalized double couple of moment $M_0=10^{10}$ Nm, occurring on the Aigio fault at (x,y) and parallel to the fault. The hydraulic response is computed as the average of pressure anomalies along the portion of the borehole intersecting the karst (see Appendix). We used a coefficient $-\partial P/\partial\varepsilon=BK_u=17$ GPa, determined from tidal analysis, and we assumed that the two Lamé coefficients λ and μ are equal to 10 GPa. The borehole intersects the fault at (0,0). The sign of the induced pressure offset depends on the position of the double–couple along the dip-direction, as explained on the graph.

the fault? A movement on the Aigio fault may induce two measurable effects on pressure record: (1) the undrained response to the coseismic stress changes and (2) the diffusion of the pressure front induced by a sudden disruption of the hydraulic barrier the fault constitutes or by a sudden dilatant damage near the fault.

3.2.1. Coseismic elastic effect

We approximate the slip on the fault by a double couple source of moment M_0. With radial coordinates (r,θ,ϕ) centered on the dislocation, the pressure disturbance induced around the source is

$$P = BK_u \frac{3M_0 \sin 2\theta \cos\phi}{4\pi r^3 \rho V_P^2} \quad (2)$$

where $BK_u=17$ GPa is the product of the Skempton coefficient and of the undrained bulk modulus and $V_P=5$ km/s is the P wave velocity of the medium.

As the Aigio fault intersects the borehole, the deformation (and hence the pressure change) induced along the borehole is heterogeneous. The pressure measured at the wellhead is shown to be the average over the section of the AIG10 borehole intersecting the karst of the induced pressure disturbance weighted by permeability along the borehole (see Appendix). As the lower karstic aquifer is extremely permeable, only the disturbances induced below the fault are considered.

Fig. 8 shows that the pressure disturbance generated by a slip with moment $M_0=10^{10}$ Nm (equivalent of a magnitude $M_w=0.6$ or a slip of 1 cm over a surface of 20 m × 20 m) reaches 60 Pa if the hypocenter is located 100 m away from the center of the borehole. An event of this magnitude is too small to be observed by the sensors located 10 km from the borehole in Trizonia. It is also too large since no sudden coseismic drop was observed on the pressure data.

The fault core has a slipping surface tilted relative to the fault plane by 37° (Fig. 9). As the gouge is 1 m thick, this suggests a slipping plane 1.3 m long. If we suppose that this is the typical dimension of the slipping surface and extrapolate scaling laws of Kanamori and Anderson [17], a typical slip on this surface would have a moment equal to $M_0=10^7$ Nm ($M_w=-1.4$). The coseismic pressure change would then be imperceptible to the pressure sensor.

The smallness of the source is compatible with the large frequencies of the hydrophone signal of Fig. 3. The corner frequency is related to the area of the source S_{source} by $f_c \simeq V_S/\sqrt{S_{source}}$ [18], where V_S is the S wave velocity. Corner frequencies for this event is close to 1 kHz.

However, if the observed pressure transient was only due to the poroelastic response to a slip on the fault, it would be instantaneous, which is not what is observed. This suggests that a slip on the fault should be still smaller, so that the sensor does not feel this poroelastic

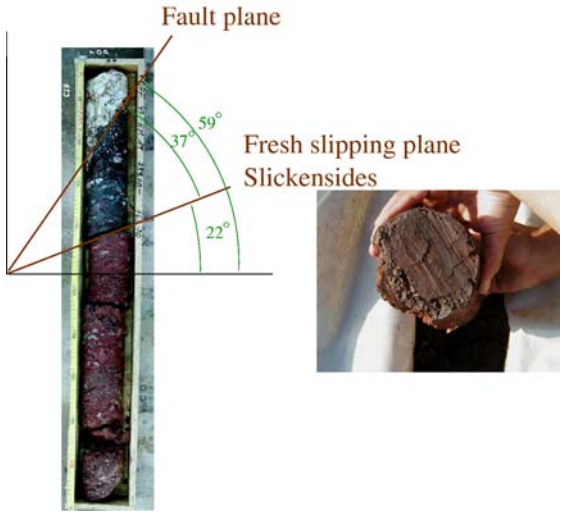

Fig. 9. Photograph of the fault core, exhibiting slickensides tilted to 37° to the plane of the Aigio fault. The box is 1 m long.

response. The signal observed would be an indirect effect.

3.2.2. Sudden removal of fluid from the karst

The long duration of the pressure transient is reminiscent of a diffusive process. For instance, let us consider the Green function in response to a sudden injection of a volume of water V at a distance R [19]. It is given by

$$p(R,t) = \frac{1}{S}\frac{V}{(4\pi Dt)^{3/2}}\exp\left(-\frac{R^2}{4Dt}\right) \quad (3)$$

where D and S are the hydraulic diffusivity and the specific storativity of the medium. This solution predicts a rapid change in pressure followed by a long recovery. This behavior is similar to the pressure drop of Fig. 2.

How can water be removed from the medium? The medium is the karst. A first possibility is that the water has left the karst. The fault acts as a hydraulic barrier separating two aquifers of different pressures. For water to leave the karst, one needs to break this seal. Cores show that slip occurred on a plane tilted relative to the fault plane (Fig. 9). This may help break the hydraulic barrier the fault constitutes. If a movement occurs on such a plane, it could open transiently a path allowing water to leave the karst to the upper aquifer.

Another possibility is that no water quits the karst but that the volume of pores is increased. Dilatancy correlated with damage induced near the fault by the slip on the fault is a possible mechanism for creation of pore volume.

If we suppose that the borehole does not disturb the propagation of the pressure front in the aquifer, the pressure observed in the borehole is the average along the section of the borehole below the fault of the disturbance described by Eq. (3). Supposing that the slip occurred on the fault plane at a distance x_0 from the intersection of the well and the borehole in the down-dip direction and at a distance y_0 in the strike direction, the recorded pressure is modeled as

$$p(t) = \frac{-\left(V\left(\mathrm{Erf}\left(\frac{x_0\cos(\phi)}{2\sqrt{Dt}}\right)+\mathrm{Erf}\left(\frac{H-x_0\cos(\phi)}{2\sqrt{Dt}}\right)\right)\right)}{8DH\pi St} \times \exp\left(-\frac{x_0^2(1-\cos(2\phi))+2y_0^2}{8Dt}\right). \quad (4)$$

$\phi = 30°$ is the angle between the borehole and the fault plane and $H = 230$ m is the length of the portion of the borehole penetrating the karst. Erf is the error function. The unknown parameters in this equation are the removed volume V and the position of the slip on the fault (x_0, y_0). Although tidal analysis provides a diffusivity value $D = 20$ m^2/s, the heterogeneous structure of the karst casts doubt on its applicability at smaller scale, and the diffusivity is also considered as unknown.

Eq. (4) gives a very satisfactory fit of the observed pressure drop (Fig. 10). The number of unknowns (3, if we impose x_0) exceeds the number of observations (2, ie the amplitude of the drop and its duration). It is thus not surprising that two very different sets of parameters fit similarly the results.

From the response of the well to the earth tides, the diffusivity of the karst was assessed to be $D \sim 20$ m^2/s. This constrains the injection of 1.7 m^3 at a distance of 350 m. The sudden passage of such a volume through the fault is improbable.

The karst is a very heterogeneous formation. At a smaller scale, the karst is better approximated as a double porosity medium, with very conductive conduits penetrating a less permeable matrix. The conduits can be seen as an extension of the borehole and are supposed to have the same homogenized pressure. The diffusion is limited by the diffusivity of the matrix. Eq. (4) should be altered to take into account the volume of the conduits but our ignorance of the karst geometry hampers this refinement. To keep Eq. (4), we suppose that the volume of the conduits is negligible. The fit of the pressure drop is then possible with much smaller removed volume. For instance, the data are compatible with the sudden injection of 1.5×10^{-3} m^3 at a distance of 20 m with a diffusivity of $D = 0.05$ m^2/s. Smaller volumes could be attained by further reducing D. With a distance of 20 m, Fig. 8 shows that the minimum magnitude that cannot

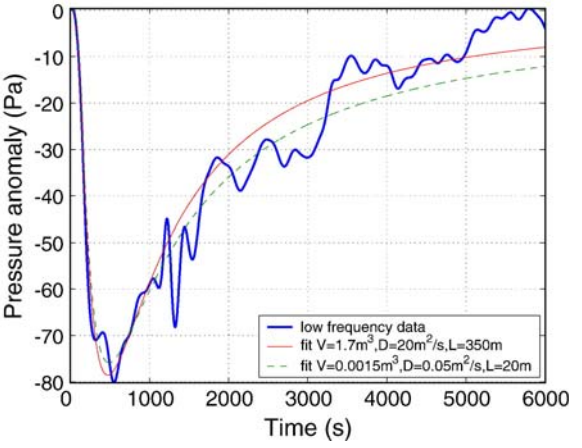

Fig. 10. The pressure data are low-passed and detrended. The pressure drop is fitted with a model in which a volume V of fluid is suddenly removed from the medium at a distance L. The karst is an aquifer with two porosities: the large cavities of the karst with a high hydraulic diffusivity $D = 20$ m^2/s, and the porous matrix with a smaller hydraulic diffusivity $D = 0.05$ m^2/s. Both cases are considered.

generate any coseismic step in pressure (less than the resolution of the sensor of 10 Pa) is only $M_0 = 10^7$ Nm ($M_w = -2$).

We conclude that the pressure drop can be modeled by dilatant damage or by the removal of fluid from the karst induced by the disruption of the hydraulic barrier the fault constitutes.

4. Conclusion

The 2003 Rat Island earthquake induced a transitory pressure drop in a well intersecting an active fault of the Corinth Rift, more than 10 000 km away. This transient of 60 Pa is to our knowledge the smallest recorded pressure anomaly triggered by the seismic waves generated by a teleseism. It is also one of the earliest, as it occurs during the passage of the S waves, which to our knowledge has not been observed before. That S waves trigger the hydraulic transient is surprising since they have also much smaller amplitude than Rayleigh waves. This suggests that the system was on the verge of unstability.

Although we lack complementary data to constrain the mechanism of the observed transient, a simultaneous high frequency event on the hydrophone installed at the wellhead suggests that the Aigio fault intersected at the borehole has slipped but with a magnitude less than −2. The pressure transient can be explained as dilatant damage or as a transient disruption of the hydraulic barrier the fault constitutes. To confirm this speculation, a complete set of sensor including several pressure transducers and hydrophones is to be installed in the well.

If confirmed, the speculated mechanism implies that the hydraulic properties of a fault can dramatically change during its slip. If the slip occurs on a structure nonparallel to the fault plane, fluid can escape very easily and prevent pressure buildup inside the fault during slip weakening mechanisms like fluid pressurization. If the slip induced dilatant damage, it would also reduce pore pressure and prevent pressurization.

Acknowledgments

We are deeply grateful to Emily Brodsky for her support and numerous fruitful discussions. We also thank Steve Hickman for his helpful suggestions. We thank an anonymous reviewer for his comments that helped to substantially improve the manuscript. The CRL development benefited from the support from the Energy Environment and Sustainable Development program of the European Commission (in particular contract no. EVR1-CT-2000-40005) and from the French CNRS (GDR-Corinth).

Appendix A. From an heterogeneous pressure field along the borehole to the wellhead pressure

Let suppose that the hydraulic anomaly of Fig. 2 is induced by a slip on the Aigio fault. The proximity of the borehole to the source raises a new problem: Eq. (4) predicts a heterogeneous pressure change along the borehole, whereas we record a single data for all the open section of AIG10.

The pressure within the well is uniform, equal to P_b. This pressure varies due to fluid exchange dV at the wall of the borehole. Its sensitivity depends on the compressibility of the fluid K_f and the volume V_b of the well:

$$dP_b = \frac{K_f}{V_b} dV \tag{A.1}$$

The incoming flux is supposed to be purely radial, so that:

$$dV = \int_{\text{open section}} 2\pi r_b \frac{C(z)}{\rho g} \frac{\partial P(r,z)}{\partial r} dz dt \tag{A.2}$$

where $P(r,z)$ is the pressure in the rock expressed in cylindrical coordinates.

The hydraulic conductivity C is linked to the permeability k by the relationship $C = \frac{\rho_f g}{\eta} k$ where ρ_f and η are the density and the dynamic viscosity of water and g is the gravity acceleration.

The pressure gradient is unknown and depends on time. For instance, if there is a sudden step in pressure in the medium surrounding the borehole, homogenization by diffusion will taper pressure discontinuity and the slope will slowly decay with time whereas a pressure front will extend. A problem arises from the absence of a characteristic distance. A typical way to solve the problem is to introduce a "skin" length, for instance the thickness of the mud cake layering the walls of the borehole after drilling. This case is implemented in the hydrological modeling software MODFLOW through the MNW module [20]. However, the intense flow experienced by the borehole during the installation of the sensor flushed this mud cake, and we have to tackle the problem differently.

Let suppose that the exponential profile can be approximated by $\frac{\partial P}{\partial r} = \frac{P(z)-P_b}{\sqrt{\kappa(z)t}}$ where $\kappa(z)$ is the local diffusivity and $P(z)$ the expected pressure along the borehole, as determined from Eq. (3). This supposes that

(1) the pressure front $\sqrt{\kappa(z)t}$, dependent on the local hydraulic diffusivity $\kappa(z)$, is small compared to the variation wavelength of $P(r,z)$, (2) and the lateral diffusion is predominant to the vertical diffusion in the medium. Combining Eqs. (A.1) and (A.2) gives the relationship of pressure in the borehole to the pressure field in the surrounding medium:

$$\frac{\partial P_b}{\partial t} = \frac{2\pi r_b K_f}{\rho g V_b} \int_{\text{open section}} C(z) \frac{P(z) - P_b}{\sqrt{\kappa(z)t}} dz$$

$$= \frac{2\pi r_b K_f}{\rho g V_b} \frac{F}{\sqrt{t}} (P_\infty - P_b) \quad (A.3)$$

with the two constants:

$$F = \int_{\text{open section}} \frac{C(z)}{\sqrt{\kappa(z)}} dz = \int \sqrt{C(z)S(z)} dz \quad (A.4)$$

$$P_\infty = \frac{\int \sqrt{C(z)S(z)} P(z) dz}{\int \sqrt{C(z)S(z)} dz} \quad (A.5)$$

$\kappa(z)=C(z)/S(z)$, where $S(z)$ is the storativity in m^{-1}. P_∞ is a weighted average of the pressure along the borehole. It crosses two different aquifers. F is estimated with the poroelastic parameters determined by tidal analysis [16]. Using the storativity of the upper aquifer of Giurgea et al. [11] $S_u=10^{-4}$ m^{-1}, the upper aquifer is found to contribute to 18% to F. This value reduces to 1.5% with a more reasonable value compatible with the expectation of poroelastic theory $S_u=\rho g\phi/K_f \sim 10^{-7}$–$10^{-6}$ m^{-1}. We will retain this choice. The karstic lower aquifer dominates the hydraulic setting of the AIG10 borehole, and F is approximated as $F \approx \sqrt{C_l S_l} H_l \sim 8.510^{-4}$ $m/s^{1/2}$, where $C_l=1.5\ 10^{-5}$ m/s, $S_l=8.4\ 10^{-7}$ m^{-1} and $H_l=240$ m are respectively the hydraulic conductivity, the storativity and the thickness intersected by the borehole of the lower aquifer.

The solution of the differential Eq. (A.3) is given as:

$$P_b(t) = P_\infty + (P_0 - P_\infty) e^{-2\sqrt{\frac{t}{\tau}}} \quad (A.6)$$

with the characteristic time $\tau = \left(\frac{\rho g V_b}{2\pi r_b K_f F}\right)^2$. The volume of the borehole equals $\pi r_b^2 H_b \approx 22$ m^3, since its radius is $r_b \approx 0.17/2$ m and its depth is $H_b=1000$ m. As $K_f \approx$ 2.2 GPa, $\tau \sim 120$ ms. This delay is much smaller than the sampling rate of our high-precision sensor (1/8 Hz), so that the pressure gauge directly measures P_∞. Note that the diffusion front will be of 3 mm to 11 cm for the upper aquifer, and of 1.2 m for the lower aquifer. In the last case, we are at the limit of our hypothesis (1) if the dislocation is close to the borehole, inducing a very heterogeneous disturbed pressure field, since $P(\sqrt{D_l t}, z)$ will differ from $P(0,z)$. However, in that case, the karst structure will render inadequate Eq. (4), which supposes a homogeneous medium. Moreover, the dislocation geometry should be also taken into account.

In conclusion, the pressure recorded by our sensor is equal to the weighted average pressure given by Eq. (A.5). It is dominated by the lower karstic aquifer. Because of our poor knowledge of the network of the karstic conduits, we cannot describe better this aquifer than as a homogeneous porous medium. Our result only gives an order of magnitude for slips on the faults very close to the borehole.

Appendix B. Supplementary data

Supplementary data associated with this article can be found, in the online version, at doi:10.1016/j.epsl.2007.03.036.

References

[1] R. Coble, The effects of Alaskan earthquake of March 27, 1964, on ground water in Iowa, Proc. Iowa Acad. Sci. 72 (1965) 323–332.

[2] D. Montgomery, M. Manga, Streamflow and water well response to earthquake, Science 300 (June 2003) 2047–2049.

[3] E. Brodsky, E. Roeloffs, D. Woodcock, I. Gall, A mechanism for sustained groundwater pressure changes induced by distant earthquakes, J. Geophys. Res. 108 (B8) (August 2003), doi:10.1029/2003GL018485.

[4] J.E. Elkhoury, E.E. Brodsky, D.C. Agnew, Seismic waves increase permeability, Nature 441 (2006) 1135–1138.

[5] E. Brodsky, S. Prejean, New constraints on mechanisms of remotely triggered seismicity at Long Valley Caldera, J. Geophys. Res. 110 (B4) (2005), doi:10.1029/2004JB00321.

[6] P. Bernard, P. Briole, B. Meyer, H. Lyon-Caen, J.-M. Gomez, C. Tiberi, C. Berge, R. Catin, D. Hatzfeld, C. Lachet, B. Lebrun, A. Deschamps, F. Courboulex, C. Laroque, A. Rigo, D. Massonet, P. Papadimitriou, J. Kassaras, D. Diagourtas, K. Makropoulos, G. Veis, E. Papazisi, C. Mitsakaki, V. Karakostas, P. Papadimitriou, D. Papanastassiou, G. Chouliaras, G. Stavrakakis, The M_s=6.2, June 15, 1995 Aigion earthquake (Greece): evidence for low angle normal faulting in the Corinth Rift, J. Seismol. 1 (1997) 131–150.

[7] I. Koukouvelas, The Egion fault earthquake-related and long-term deformation, Gulf of Corinth, Greece, J. Geodyn. 26 (2–4) (1998) 501–513.

[8] A. Avallone, P. Briole, A. Agatza-Balodimou, H. Billiri, O. Charade, C. Mitsakaki, A. Nercessian, K. Papazissi, D. Paradissis, G. Veis, Analysis of eleven years of deformation measured by GPS in the Corinth Rift Laboratory area, C. R. Geosci. 336 (4–5) (March 2004) 301–311.

[9] D. Pantosti, P.M. De Martini, I. Koukouvelas, L. Stamatopoulos, N. Palyvos, S. Pucci, F. Lemeille, S. Pavlides, Paleoseismological investigations of the Aigion fault (Gulf of Corinth, Greece), C. R. Géosci. 336 (4–5) (2004) 335–342.
[10] F.H. Cornet, M.L. Doan, I. Moretti, G. Borm, Drilling through the active Aigion fault: the AIG10 well observatory, C. R. Géosci. 336 (4–5) (2004) 395–406.
[11] V. Giurgea, D. Rettenmaier, L. Pizzino, I. Unkel, H. Hötzl, A. Förster, F. Quattrocchi, Preliminary hydrogeological interpretation of the Aigion area from the AIG10 borehole data, C. R. Géosci. 336 (4–5) (2004) 467–475.
[12] M. West, J. Sánchez, S. McNutt, Periodically triggered seismicity at Mount Wrangell, Alaska, after the Sumatra earthquake, Science 308 (2005) 1144–1146.
[13] S. Sil, J.T. Freymueller, Well water level changes in Fairbanks, Alaska, due to the great Sumatra–Andaman earthquake, Earth Planets Space 58 (2) (2006) 181–184.
[14] M. Miyazawa, J. Mori, Evidence suggesting fluid flow beneath Japan due to periodic seismic triggering from the 2004 Sumatra–Andaman earthquake, Geophys. Res. Lett. 33 (2006) L05303, doi:10.1029/2005GL025087.
[15] S. Hurwitz, M.J. Johnston, Groundwater level changes in a deep well in response to an intrusion event on Kilauea volcano, Hawai'i, Geophys. Res. Lett. 30 (22) (2003), doi:10.1029/2003GL018676.
[16] Doan, M., 2005. Étude in-situ des interactions hydromécaniques entre fluides et failles actives — application au Laboratoire du Rift de Corinthe. PhD Thesis, Institut de Physique du Globe de Paris.
[17] H. Kanamori, D.L. Anderson, Theoretical basis of some empirical relations in seismology, Bull. Seismol. Soc. Am. 65 (5) (1975) 1073–1095.
[18] R.E. Abercrombie, Earthquake source scaling relationships from −1 to 5 M_L using seismograms recorded at 2.5-km depth, J. Geophys. Res. 100 (B2) (1995) 24015–24036.
[19] H.F. Wang, Theory of Linear Poroelasticity with Applications to Geomechanics and Hydrogeology, Princeton Series in Geophysics, Princeton University Press, Princeton, NJ, 2000.
[20] Halford, K., Hanson, R., 2002. User guide for the drawdown-limited, multinode well (MNW) package for the U.S. Geological Survey's modular three-dimensional finite-difference groundwater flow model, versions MODFLOW-96 and MODFLOW-2000. Tech. Rep. 02-293, U.S. Geological Survey.